The pro-inflammatory peptide LL-37 promotes ovarian tumor progression through recruitment of multipotent mesenchymal stromal cells

Seth B. Coffelt[a], Frank C. Marini[b], Keri Watson[b], Kevin J. Zwezdaryk[c], Jennifer L. Dembinski[b], Heather L. LaMarca[d], Suzanne L. Tomchuck[c], Kerstin Honer zu Bentrup[c], Elizabeth S. Danka[c], Sarah L. Henkle[c], and Aline B. Scandurro[c,1]

[a]Tumor Targeting Group, University of Sheffield School of Medicine, Sheffield, United Kingdom; [b]Department of Stem Cell Transplant and Cellular Therapy, University of Texas M. D. Anderson Cancer Center, Houston, TX; and [c]Department of Microbiology and Immunology, Tulane University, New Orleans, LA; and [d]Department of Molecular & Cellular Biology, Baylor College of Medicine, Houston, TX

Communicated by Darwin J. Prockop, Tulane University, New Orleans, LA, January 9, 2009 (received for review April 22, 2008)

Bone marrow-derived mesenchymal stem cells or multipotent mesenchymal stromal cells (MSCs) have been shown to engraft into the stroma of several tumor types, where they contribute to tumor progression and metastasis. However, the chemotactic signals mediating MSC migration to tumors remain poorly understood. Previous studies have shown that LL-37 (leucine, leucine-37), the C-terminal peptide of human cationic antimicrobial protein 18, stimulates the migration of various cell types and is overexpressed in ovarian, breast, and lung cancers. Although there is evidence to support a pro-tumorigenic role for LL-37, the function of the peptide in tumors remains unclear. Here, we demonstrate that neutralization of LL-37 in vivo significantly reduces the engraftment of MSCs into ovarian tumor xenografts, resulting in inhibition of tumor growth as well as disruption of the fibrovascular network. Migration and invasion experiments conducted in vitro indicated that the LL-37-mediated migration of MSCs to tumors likely occurs through formyl peptide receptor like-1. To assess the response of MSCs to the LL-37-rich tumor microenvironment, conditioned medium from LL-37-treated MSCs was assessed and found to contain increased levels of several cytokines and pro-angiogenic factors compared with controls, including IL-1 receptor antagonist, IL-6, IL-10, CCL5, VEGF, and matrix metalloproteinase-2. Similarly, Matrigel mixed with LL-37, MSCs, or the combination of the two resulted in a significant number of vascular channels in nude mice. These data indicate that LL-37 facilitates ovarian tumor progression through recruitment of progenitor cell populations to serve as pro-angiogenic factor-expressing tumor stromal cells.

FPRL1 | hCAP-18 | mesenchymal stem cell | ovarian cancer | tumor engraftment

Histological examination of ovarian, breast, and lung tumors has shown that the pro-inflammatory peptide LL-37 (leucine, leucine-37) is up-regulated in these malignancies (1–3). LL-37 was originally identified as a component of host defense peptides released by innate immune cells to combat microorganisms (4–6). However, recent investigations have revealed more complex and diverse functions of the peptide (7–9). LL-37 is synthesized as the 37-aa C terminus of human cationic antimicrobial protein 18 (hCAP-18) and maintained in an inactive state until release by enzymatic cleavage (4, 5, 10–12). Expression and secretion of LL-37 is elevated at sites of inflammation and wound healing, where the peptide functions as a proliferative signal and pro-angiogenic factor (7–9). The peptide also acts as a potent chemoattractant for various immune cells through activation of formyl peptide receptor like-1 (FPRL1) (13, 14). In contrast to LL-37's established functions in host defense and tissue damage, the role of the peptide in the tumor microenvironment and the advantage given to tumor cells by its overexpression is not entirely clear.

The heterogeneous population of progenitor cells known as multipotent stromal cells or mesenchymal stem cells (MSC) has been shown to engraft within tumor microenvironments, where they incorporate into the stroma of solid tumors as tumor-associated fibroblasts or pericyte-like cells and potentiate tumor progression through the release of paracrine signals (15–25). Kaposi sarcoma seems to be the only exception to this phenomenon, as MSCs inhibit the growth of this tumor type (23). However, the tropism of MSCs for Kaposi sarcoma is maintained, suggesting that the factors responsible for MSC recruitment to tumors are commonly secreted by multiple tumors of different tissue origin. In fact, a number of soluble factors have been implicated in MSC migration to tumors, including many of the same inflammatory mediators up-regulated in injured and inflamed tissues (17, 18, 20, 26–28). Therefore, given the similar expression pattern of LL-37 in tumors, damaged tissue, and inflammation, where MSCs are prominent, as well as the ability of the peptide to stimulate chemotaxis of various cell types, we hypothesized that ovarian tumor-derived LL-37 recruits MSCs to the tumor microenvironment to support cancer progression.

Results

LL-37 Promotes Migration and Invasion of MSC in Vitro. As LL-37 has been shown to activate migration through the FPRL1 receptor in various cell types, several donor pools of MSCs were examined for expression of FPRL1 (13). Flow cytometry analyses confirmed the expression of FPRL1 on all MSC donor pools, corroborating results from other laboratories (Fig. 1*A*) (29).

We extended our previous findings to determine the optimal dosage of the peptide using in vitro chemotaxis assays (26). As shown in Fig. 1*B*, LL-37 induced the migration of MSCs in a dose-dependent manner, and the peptide performed as well as EGF, an established chemotactic factor for these cells (17). MSCs were pretreated with pertussis toxin (Ptx), a $G_{\alpha i}$ inhibitor, before activation with LL-37 or EGF to prevent FPRL1 signaling. Ptx treatment followed by LL-37 stimulation resulted in a significant inhibition of MSC migration, whereas no significant difference was observed between EGF-stimulated, Ptx-treated cells and EGF-stimulated cells alone (Fig. 1*C*). LL-37 and EGF were also preincubated with a neutralizing LL-37 antibody and, as expected, the neutralizing antibody (αLL-37) abolished LL-37's chemotactic effects on MSCs but had no effect on EGF-stimulated cells (Fig. 1*C*). No decrease in MSC migration was observed in wells with a control IgG antibody (data not shown).

MSC invasion through Matrigel-coated inserts was also sig-

Author contributions: S.B.C., F.C.M., K.J.Z., and A.B.S. designed research; S.B.C., F.C.M., K.W., K.J.Z., J.L.D., H.L.L., S.L.T., K.H.z.B., E.S.D., S.L.H., and A.B.S. performed research; S.B.C., F.C.M., K.J.Z., H.L.L., S.L.T., and A.B.S. analyzed data; and S.B.C., F.C.M., and A.B.S. wrote the paper.

The authors declare no conflict of interest.

[1]To whom correspondence should be addressed. E-mail: alibscan@tulane.edu.

This article contains supporting information online at www.pnas.org/cgi/content/full/0900244106/DCSupplemental.

www.pnas.org/cgi/doi/10.1073/pnas.0900244106

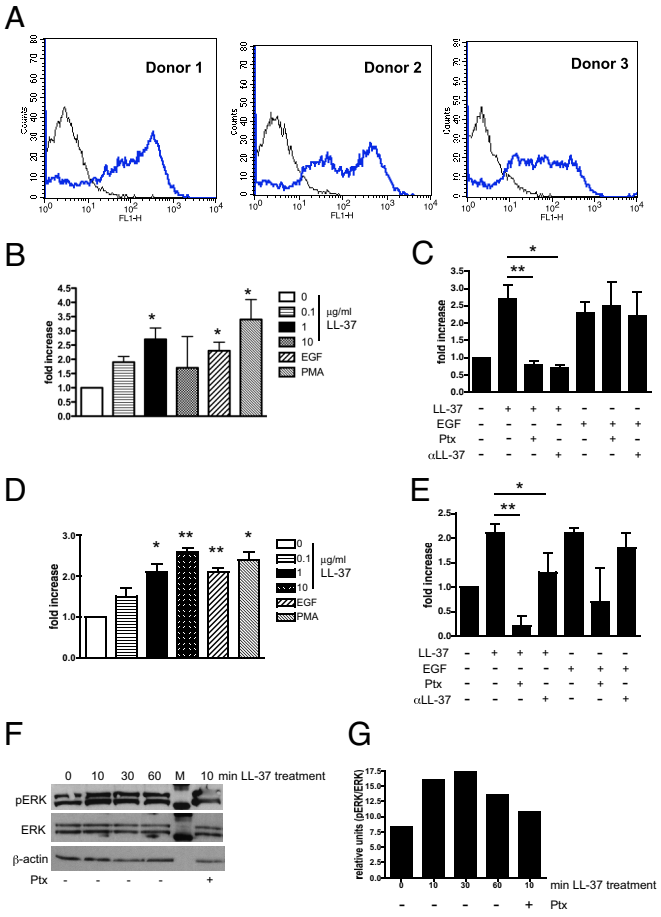

Fig. 1. LL-37 mediates MSC migration and invasion through a G protein-coupled receptor. (*A*) FPRL1 expression on 3 different donor pools of MSCs analyzed by flow cytometry. (*B*) Graphic representation of MSC migration stimulated as indicated in a modified Boyden chamber. EGF and PMA were used at 10 ng/mL. (*C*) MSC migration after pretreatment of cells with 100 ng/mL pertussis toxin (Ptx), or preincubation of LL-37 and EGF with an anti-LL-37 neutralizing antibody (αLL-37). (*D*) Invasion of MSCs through Matrigel-coated inserts following stimulation as indicated. (*E*) MSC invasion after pretreatment of cells with Ptx or preincubation of LL-37 and EGF with αLL-37 antibody. *, $P < 0.05$; **, $P < 0.01$. (*F*) Lysates from LL-37-treated MSCs analyzed for ERK phosphorylation by Western blot. MSCs in the far right lane were pretreated with Ptx for 1 h before stimulation with LL-37 for 10 min. M = molecular weight marker. (*G*) Quantification of Western blot band intensity by densitometry ($n = 3$), plotted as a bar graph.

nificantly enhanced by LL-37 stimulation (Fig. 1*D*). Pretreatment of MSC with Ptx significantly attenuated LL-37's ability to promote invasion (Fig. 1*E*). EGF-stimulated cells were slightly affected by Ptx, but this was not significant. The anti-LL-37 antibody (αLL-37) significantly blocked LL-37 from binding to MSC surface receptors, as MSCs in this experimental group did not invade as effectively (Fig. 1*E*). By contrast, the anti-LL-37 antibody did not affect EGF stimulation of MSC invasion. An IgG control antibody did not interfere with the ability of LL-37 or EGF to induce MSC invasion (data not shown). Taken together, these data suggest that LL-37 induces MSC trafficking through a $G_{\alpha i}$-coupled receptor, such as FPRL1.

As further validation of FPRL1 involvement in LL-37-mediated responses, MSCs were assessed for activation of signaling molecules downstream of this receptor. Western blot analysis of MSC lysates showed that ERK-1 and -2 are robustly phosphorylated beginning 10 min after LL-37 treatment and maintained over 60 min (Fig. 1 *F* and *G*). However, MSCs pretreated with Ptx before stimulation by LL-37 reduced ERK-1/2 activation, providing further evidence in support of notion that LL-37 stimulates MSCs through FPRL1.

The growth kinetics of MSCs were then analyzed after treatment with increasing doses of recombinant LL-37 in the presence of serum. After a 72-hour time course, LL-37 failed to stimulate the proliferation of MSCs (data not shown).

Tumor-Derived LL-37 Functions as a Chemoattractant for MSCs in Vivo. To assess the importance of LL-37 in recruitment of MSCs to tumors, an in vivo migration assay was used. Human tumor xenografts were established in SCID mice by injection of OVCAR-3 ovarian cancer cells, whose expression of hCAP-18/LL-37 was previously reported (1). After 3.5 weeks, mice were randomly divided into 2 groups. One group ($n = 11$) was given an IgG control antibody and the other group ($n = 14$) was given an anti-LL-37 antibody to neutralize the peptide's effect before injection of firefly luciferase (ffLUC)-labeled MSCs. Bioluminescence images were taken throughout the experiment to monitor engraftment of MSCs into the developing ovarian tumors. Neutralization of tumor-derived LL-37 in anti-LL-37 antibody-treated animals (αLL-37) abrogated the number of engrafted MSCs into tumors compared with IgG-treated animals (Fig. 2*A*). Bioluminescence from engrafted MSCs was quantified, and a significant difference was observed between IgG-treated animals and anti-LL-37-treated animals for each day an image was taken (Fig. 2*B*).

At the end of the experiment, tumors were analyzed via immunohistochemical staining to confirm the reduced MSC engraftment into tumors of anti-LL-37-treated animals. MSCs were identified with an anti-ffLUC antibody, and their engraftment into the tumor stroma as fibroblast-like cells was readily observed (Fig. 2 *C* and *D*; white arrows). The difference in overall MSC engraftment between IgG- and anti-LL-37-treated was evident in these representative sections, validating bioluminescence imaging. In addition to ffLUC, tumor sections were co-stained for expression of LL-37. Tumor cells of IgG-treated mice expressed measurable levels of hCAP-18/LL-37, whereas expression of the peptide was dramatically reduced in tumors of anti-LL-37-treated mice (Fig. 2*C*). Surprisingly, co-localization of ffLUC and LL-37 was noted in tumor-infiltrating MSCs and, when compared with tumor cells, MSCs expressed considerably higher levels of hCAP-18/LL-37 (Fig. 2 *C* and *F*). MSCs were also noted in perivascular regions neighboring vessels, indicative of pericyte-like differentiation of these cells (Fig. 2*F*).

Neutralization of Tumor-Derived LL-37 Reduces Tumor Growth. Of the 11 tumor-bearing animals that received the IgG control antibody, 10 animals had visible tumors upon sacrifice. By contrast, 5 of the 14 animals given the anti-LL-37 antibody treatment regimen had no detectable tumor mass. Tumors from both groups were weighed after surgical removal and those from IgG-treated animals were significantly larger than those from anti-LL-37-treated animals (98.43 ± 13.51 mg vs. 46.39 ± 12.65 mg, respectively; Fig. 3*A*). To confirm these observations, tumors were stained for the proliferation marker Ki-67. A dramatic difference was again noted between tumors from IgG- and anti-LL-37-treated animals. Tumor nuclei of IgG-treated mice were almost all positive for Ki-67, in contrast to the few positive nuclei in tumors from LL-37 antibody-treated mice (Fig. 3*B*). Quantification of Ki-67$^+$ nuclei in both treatment groups revealed a statistically significant difference (Fig. 3*C*). Notably, the stromal components of tumors from anti-LL-37-treated mice, including fibroblasts and endothelial cells, were absent in a large majority of areas (Fig. 3*B*; yellow arrows). Necrotic regions were also common in tumors from anti-LL-37-treated animals, but not in IgG-treated tumors. As shown in Fig. 3*D*, these necrotic areas stained positively for LL-37, suggesting that the peptide is

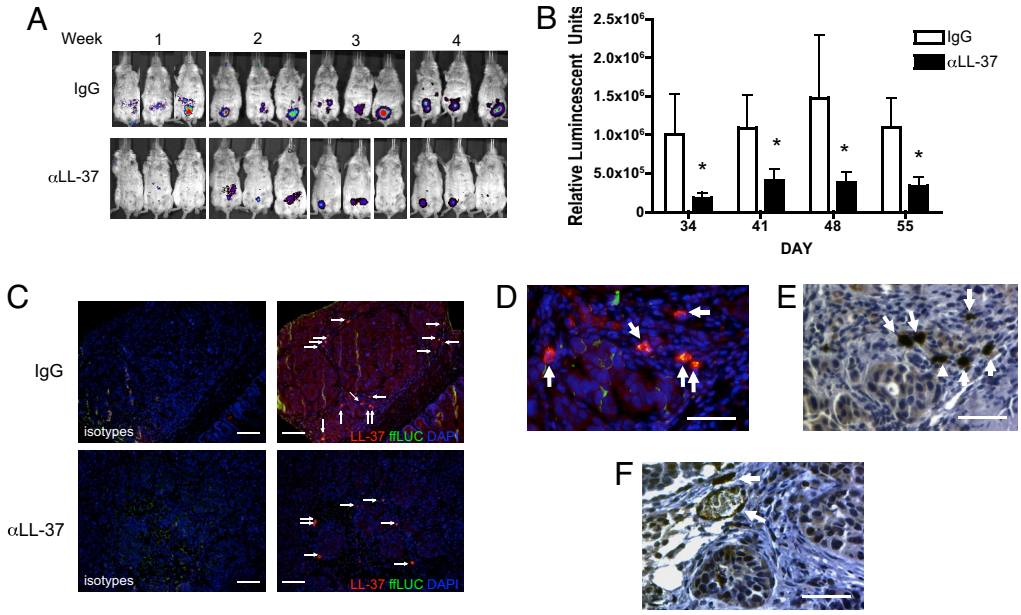

Fig. 2. Inhibition of LL-37 significantly reduces engraftment of MSCs into ovarian tumors. Human ovarian tumor xenografts were established i.p. in SCID mice. Mice were treated with IgG or anti-LL-37 antibodies (αLL-37) twice a week for 4 weeks. ffLUC-labeled MSCs were injected 4 times at weekly intervals 1 day after the first weekly injection of antibody, then visualized by bioluminescence in live mice. (*A*) Representative images of MSC engraftment into ovarian tumors 7 days after each injection of MSC. (*B*) Quantification of luminescence units emanating from tumor-engrafted MSCs. Values are mean ± SE. $*P < 0.05$. (*C*) Expression of LL-37 (red) in ovarian tumor sections of IgG- and αLL-37-treated mice. MSCs were identified using an anti-ffLUC antibody (green) and are indicated by white arrows. Nuclei were detected with DAPI. Sections are magnified ×100. (Scale bar, 100 μm.) (*D*) High-powered image (×400) of tumor section fluorescently labeled as described. (*E*) Sequential section of *D* immunohistochemically stained with anti-LL-37 antibodies followed by hematoxylin counterstain. (*F*) Example of LL-37-expressing MSCs in perivascular areas. (Scale bar, 50 μm, *D–F*.)

sequestered in the debris. Taken together, these data strongly implicate a pro-tumorigenic role for tumor-derived LL-37 through its recruitment of progenitor cell populations capable of differentiating into supportive stromal cells.

MSC Exposure to LL-37 Promotes Secretion of Angiogenic and Inflammatory Molecules. It is well established that MSCs produce many trophic factors with pro-tumorigenic functions (19, 26, 30). Evidence from the in vivo experiments described here indicated that MSCs also produce LL-37. We tested conditioned medium from several MSC donor pools growing in culture by ELISA and found that these cells readily secrete the peptide (Fig. 4*A*).

Next, we set out to determine how tumor-infiltrating MSCs would react to the LL-37-rich microenvironment of ovarian tumors. We have previously reported that LL-37 enhances the secretion of IL-1β, IL-6, IL-8, IL-10, and TNF-α from MSC while diminishing the secretion of IL-12 (p70) (26). To identify additional MSC-derived cytokines and growth factors that may be regulated by ovarian tumor-derived LL-37 and expand our previous findings, conditioned medium from various LL-37-treated MSC donor pools was analyzed by Luminex-based assays. After 48 h of LL-37 treatment, MSCs were stimulated to release significantly more of the following cytokines compared with untreated cells: IL-1 receptor antagonist, IL-6, IL-10, CCL5 (regulated upon activation, normal T cell expressed and secreted; RANTES), and VEGF (Fig. 4*B*).

Conditioned medium was also analyzed for the presence and activation of matrix metalloproteinases (MMPs) by zymography assays. Untreated MSCs secreted large amounts of the MMP-2 pro-form; no noticeable difference in expression was noted in the MMP-2 pro-form, regardless of treatment (Fig. 4*C Upper*). However, enzymatic activity of the active form of MMP-2 was increased after treatment of MSCs with LL-37, EGF, and phorbol myristate acetate (PMA; Fig. 4 *C* and *D Lower*). MMP-9 activity was undetectable after any treatment, and no expression was noted in casein gels, indicating that MSCs do not secrete measurable levels of stromelysins such as MMP-3 (data not shown).

We tested whether conditioned medium from LL-37-treated MSCs could increase endothelial cell tubule formation in vitro. Serum-starved human umbilical vein endothelial cells (HUVECs) were seeded onto growth factor-reduced Matrigel in the presence of MSC-conditioned medium. As shown in Fig. 4*E*, all 3 donor pools of LL-37-treated MSC-conditioned medium stimulated HUVECs to form tubules at a faster rate than medium from untreated MSCs. HUVECs exposed to medium from LL-37-treated MSCs began to migrate and organize into tube-like structures after only 2 hours. These data not only confirmed that LL-37-treated MSC-conditioned medium con-

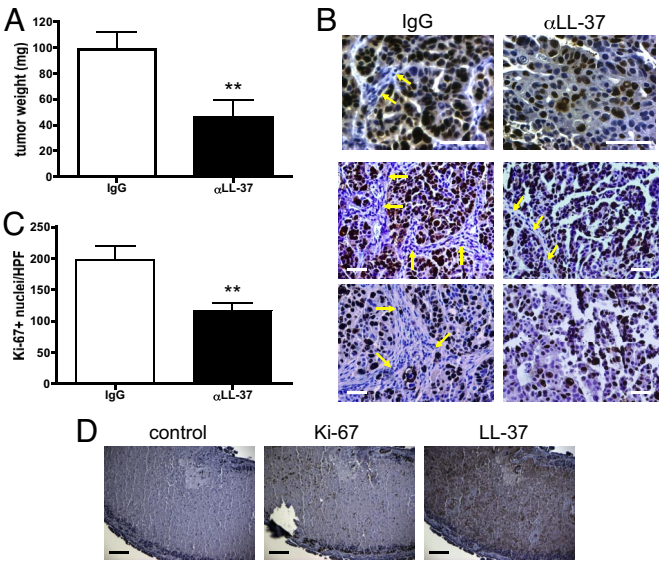

Fig. 3. Growth of ovarian tumor xenografts is diminished by neutralization of LL-37. (*A*) Graphic representation of tumor weights from IgG- ($n = 10$) and αLL-37-treated ($n = 9$) animals obtained after surgical removal. Values are mean ± SE. **, $P < 0.01$. (*B*) Representative images of tumors stained for Ki-67 with hematoxylin counterstain. Arrows indicate mouse stroma in human xenograft tumors. (Scale bar, 50 μm.) (*C*) Graphic representation of the average number of Ki-67$^+$ nuclei per high-powered field. Values are mean ± SE. **, $P < 0.01$. (*D*) Expression of Ki-67 and LL-37 in tumor necrotic region from an αLL-37-treated mouse. (Scale bar, 100 μm.)

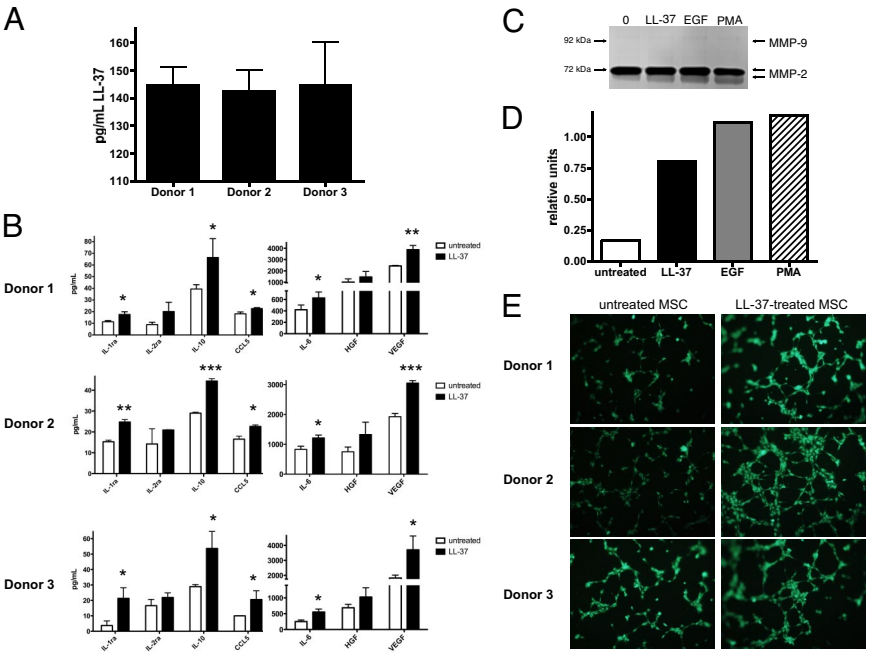

Fig. 4. MSCs secrete increased levels of angiogenic and inflammatory mediators after LL-37 stimulation. (*A*) The concentration of LL-37 in conditioned medium taken from unstimulated MSCs in culture. (*B*) Serum-starved MSCs were treated with 5 μg/mL LL-37 for 48 h, then conditioned medium was analyzed by Luminex-based cytokine arrays. Values are mean ± SE. *, $P < 0.05$, **, $P < 0.01$. (*C*) Analysis of MSC-conditioned medium after treatment for 48 h as indicated by gelatin zymography. The representative image depicts the electrophorectic pro-MMP-2 (72 kDa) and active MMP-2 (62 kDa). MMP-9 (92 kDa) was not undetectable. (*D*) Quantification of zymography by densitometry. Intensity of the lower band (active MMP-2, 62 kDa) is plotted as a bar graph ($n = 3$). (*E*) Conditioned medium from untreated and LL-37-treated MSCs was added to HUVECs, then seeded onto Matrigel. Fluorescently labeled cells were monitored were for formation of capillary-like tubules. Photographs are representative of HUVECs after 2 h incubation.

tains increased amounts of pro-angiogenic molecules, they also confirmed that the pro-angiogenic milieu is functional and has bioactivity.

LL-37 Enhances the Pro-Angiogenic Activity of MSC. Because MSCs secreted larger amounts of pro-angiogenic factors in response to LL-37, we hypothesized that tumor-associated MSCs are stimulated in the same manner by a microenvironment abundant in LL-37. To this end, serum-starved MSCs were mixed into Matrigel with and without growth factors, and then injected into the flanks of nude mice. LL-37, as well as the combination of basic FGF2 and VEGF, were added to Matrigel without cells as controls. Matrigel plugs containing growth factors, but no cells, induced a significant number of vascular channels compared with plugs without growth factors (Fig. 5 *A* and *B*). Surprisingly, the stimulation of angiogenesis by LL-37 exceeded that of the FGF2/VEGF combination at the concentrations used here. MSCs, on their own, induced a similar response as FGF2/VEGF. The numbers of vascular channels in Matrigel plugs with MSC and LL-37 were significantly greater than those containing MSCs alone or MSCs and FGF2/VEGF. However, there was no synergistic or additive effect on angiogenesis in plugs containing MSCs and growth factors, as we had anticipated. MSCs with either LL-37 or FGF2/VEGF did not significantly increase the number of vascular channels compared with plugs without cells. These data implicate dual functions for LL-37: activation of MSC as well as murine endothelial cells.

As shown in Fig. 5*C*, by using Ki-67 to identify human cells, MSCs were observed around endothelial cells, but did not incorporate into the vasculature, suggesting pericyte-like differentiation and corroborating our previous reports (18, 27). We investigated LL-37's effect on the pericyte-like differentiation of MSCs by tubule formation assay. Serum-starved MSCs were seeded onto Matrigel and treated with LL-37 or FGF2 or left untreated. LL-37 stimulated MSCs to form organized, capillary-like structures in the same manner as FGF2 treatment, whereas MSCs without growth factor influence remained as single-cell entities, indicating that LL-37 may be involved in differentiation of MSCs into pericytes in tumors (Fig. 5*D*).

Discussion

Emerging evidence indicates that inflammatory molecules play a pivotal role in tumor progression; however, the function of many of these tumor-derived inflammatory mediators remains poorly understood (31). Herein, we demonstrate that LL-37 promotes ovarian tumor progression through recruitment and engraftment of MSCs into tumors, where these cells provide pro-angiogenic and immunomodulatory factors to support tumor growth and progression.

This study directly tested the importance of a tumor-derived MSC chemotactic factor by using an in vivo assay. Previous reports from our laboratory and others suggest that additional chemokines, growth factors, and danger signals may be involved in MSC migration to tumors (17, 18, 20, 26, 27). Thus, it is unlikely that LL-37 is acting alone in the recruitment of MSCs to the tumor microenvironment given the vast production of chemotactic factors by tumor and stromal cells. In support of this notion, neutralization of LL-37 in tumor-bearing animals did not completely block MSC engraftment. Additionally, few chemokine receptors have been implicated in this process. Our recent data suggest that CCR2—the receptor for CCL2 (also called monocyte chemotactic protein 1)—is involved, as incubation of murine MSCs with anti-CCR2 blocking antibodies decreases migration of these cells (18). The data presented here indicate that LL-37 mediates MSC migration through FPRL1.

Exogenously delivered MSC incorporated into tumor stroma and maintained a fibroblast appearance or differentiated into pericyte-like cells—observations consistent with our previous reports and those of others (15–20, 23, 32–34). However, the inhibition of MSC engraftment into tumors resulted in disorganization of the fibrovascular network, strongly suggesting a critical role for LL-37 in recruitment of progenitor populations that serve as carcinoma-associated fibroblasts and pericytes. Our data suggest that MSCs, when resident in LL-37-rich tumors, are activated to release trophic factors that initiate angiogenesis and/or differentiate into blood vessel-supporting cells. Although evidence of this pro-angiogenic effect was presented here, the importance of the increased cytokine levels, such as IL-10 and CCL5, in response to LL-37 was not explored in this study. Other reports have shown that MSCs possess an innate ability to modulate the function of various immune cell

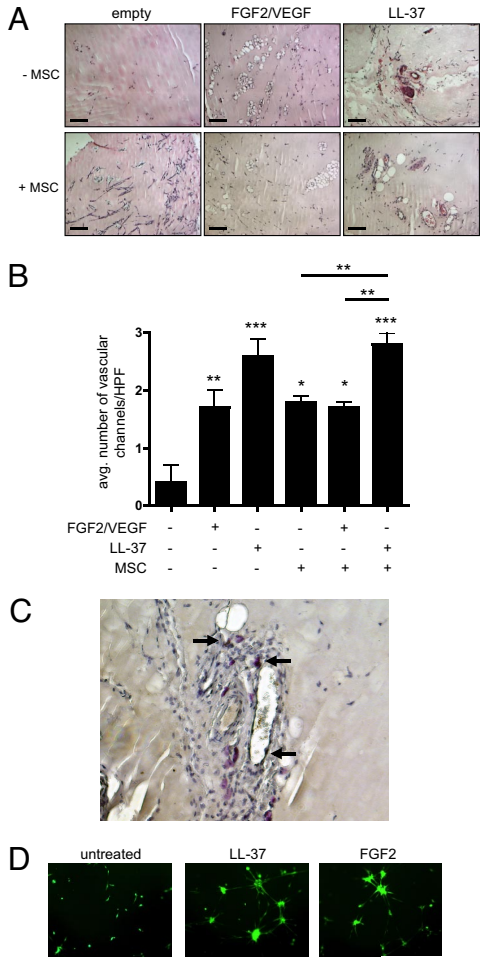

Fig. 5. LL-37 enhances the pro-angiogenic activity of MSCs. (*A*) LL-37 or the combination of FGF and VEGFA was added to cold Matrigel with or without MSCs and injected into nude mice ($n < 6$). The absence of growth factors and cells served as negative control. After 7 to 10 days, Matrigel plugs were surgically removed, fixed, sectioned, and stained by H&E. Representative images of vascular channels are shown. (Scale bar, 100 μm.) (*B*) The average number of vascular channels in each plug section was determined by counting 3 high-powered fields of view then graphically represented. Values are mean ± SE. *, $P < 0.05$, **, $P < 0.01$, ***, $P < 0.001$. (*C*) Example of MSCs in perivascular areas identified by Ki-67 staining. (*D*) Fluorescently labeled, serum-starved MSCs were seeded onto Matrigel in the presence of 5 μg/mL LL-37 or 10 ng/mL FGF2 and allowed to incubate overnight. Formation of tubules, indicative of their pericyte-like differentiation, was captured by microscopy at ×200 the next day.

populations via these factors (35, 36). Another effect of LL-37 on MSCs was the elevated secretion of CCL5. MSCs have been shown to promote breast cancer metastases through release of this cytokine, raising the possibility that LL-37 may be the instigator in this process (19).

Unexpectedly, staining for LL-37 in ovarian tumor xenograft sections proved a better identifier of MSCs than ffLUC. As noted in Fig. 2, LL-37 expression was much higher in MSCs than ovarian cancer cells, indicating that both tumor cells and MSCs contribute the peptide to the cytokine milieu of the tumor. This increase in total LL-37 levels may then lead to recruitment of more MSCs perpetuating the progression of the tumor. Perivascular MSCs may also influence endothelial cells through secretion of LL-37, as the peptide's effects on endothelial cells has already been established through FPRL1 activation (7).

The results presented here and in previous reports suggest the following sequence of events summarized in Fig. 6: (*i*) genetic

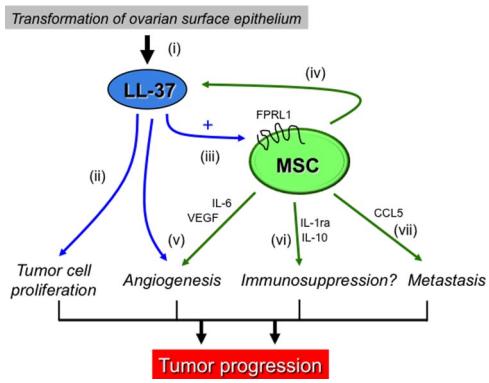

Fig. 6. Schematic illustration of effects of LL-37 and MSCs on ovarian tumor progression (see *Discussion*).

alterations in ovarian surface epithelial cells or other tissues elevates expression of LL-37, a peptide whose expression is low or absent in normal cells (1); (*ii*) LL-37 feeds back on the tumor epithelium, stimulating epithelial cell proliferation (1–3); (*iii*) LL-37 activates the MSC population to migrate into the tumor mass and enhances MSC secretion of pro-angiogenic factors; (*iv*) MSCs provide additional LL-37 to the tumor microenvironment; (*v*) LL-37 as well as other tumor- and MSC-derived molecules induce angiogenesis as the tumor expands; (*vi*) MSC produce immunosuppressive factors, likely in response to the LL-37-rich microenvironment, that function to dampen anti-tumor immunity; and (*vii*) cytokines such as CCL5 released by LL-37-stimulated MSCs enable an invasive phenotype from tumor cells. The overall consequence of LL-37's actions through its recruitment of MSCs is advancement of tumor progression.

Materials and Methods

More detailed methods are presented in *SI Materials and Methods*.

Cell Culture. Human MSC were obtained from Tulane University's Center for Gene Therapy (New Orleans, LA) and Lonza/Cambrex (Walkersville, MD). The cells were characterized by flow cytometry and various differentiation assays, and the cells were propagated as described (26, 27). MSC were used at passages no greater than 5. OVCAR-3 ovarian cancer cells were cultured as described in ref. 1.

Flow Cytometry. Anti-FPRL1 antibodies or isotype controls were detected with Alexa-488-conjugated goat anti-rabbit secondary antibodies.

Boyden Chamber Migration Assay. Chemoattractants with and without an anti-LL-37 neutralizing antibody was added to the lower compartment of a 48-well modified Boyden chamber. Serum-starved MSC were added to the upper chamber. Where indicated, MSC were pretreated with 100 ng/mL pertussis toxin (Ptx).

Invasion Assay. The assay was performed in a similar manner to migration assays using inserts coated with growth factor-reduced Matrigel.

Western Blot Analysis. LL-37-treated MSC lysates were electrophoresed and transferred to nitrocellulose membranes. Quantification of band intensity was performed using National Institutes of Health ImageJ software.

In Vivo Migration Assay. Female SCID/CB17 mice were injected i.p. with OVCAR-3 ovarian cancer cells and tumors were allowed to establish for 3.5 weeks. After this time, half the mice were treated with 50 μg of nonspecific mouse IgG antibodies or 50 μg of anti-LL-37 antibodies. Antibodies were given twice a week for the duration of the experiment. MSC were infected with 500 viral particles per cell of Ad-ffLUC-RDG, 24 h before injection. D-Luciferin was used to detect MSC, 7 d after MSC injections. Bioluminescent images were acquired from anesthetized mice with the IVIS-Xenogen system (Caliper Life Sciences, Hopkington, MA), and photons per second were measured in regions of interest using Living Image software.

Histology and IHC. Tumors were fixed in formalin solution and embedded in paraffin. Sections were stained with hematoxylin and eosin. Immunofluorescence staining for LL-37 and firefly luciferase (ff-LUC) was performed using Alexa-488- and Alexa-568-conjugated antibodies, respectively. IHC was performed as previously described using Dako's Animal Research Kit (1). Images were evaluated using a Zeiss Axioplan 2 fluorescence microscope and Intelligent Innovations software (SlideBook version 4).

Analysis of MSC-Secreted Soluble Factors. MSC-conditioned medium was analyzed by a luminex-based assay. Zymography assays were performed as before (1). Quantification of band intensity was performed using ImageJ software.

Tubule Formation Assay. HUVECs were resuspended in MSC-conditioned medium and seeded onto Matrigel then fluorescently labeled. For MSC differentiation on Matrigel, cells were treated with LL-37 or FGF2.

Matrigel Plug Assay. Female BALB/c nude mice ($n = 14$) were used as described in ref. 27. Matrigel was loaded with LL-37 (final volume = 5 μg/mL), FGF2/VEGF (final volume = 10 and 25 ng/mL, respectively), and 2.5×10^5 MSC when appropriate. Vascular channels were identified from H&E stained sections and the average number from 3 separate 400× fields was calculated for each plug.

Statistical Analyses. Student's *t* test or one-way ANOVA followed by Newman-Keuls post hoc test was used for *P* values.

ACKNOWLEDGMENTS. We thank Dr. Jeff Rosen and his team for their accommodation and Dr. Cindy Morris for the HUVECs. This work was supported in part by National Institutes of Health grants 1P20RR20152–01 (to A.B.S.) and CA-1094551, CA-116199, and CA49639 (to F.C.M.); Susan G. Komen Breast Cancer Foundation grant BCTR0504372 (to K.W., J.L.D., and F.C.M.), and the W. M. Keck Foundation.

1. Coffelt SB, et al. (2008) Ovarian cancers overexpress the antimicrobial protein hCAP-18 and its derivative LL-37 increases ovarian cancer cell proliferation and invasion. *Int J Cancer* 122:1030–1039.
2. Heilborn JD, et al. (2005) Antimicrobial protein hCAP18/LL-37 is highly expressed in breast cancer and is a putative growth factor for epithelial cells. *Int J Cancer* 114:713–719.
3. von Haussen J, et al. (2008) The host defence peptide LL-37/hCAP-18 is a growth factor for lung cancer cells. *Lung Cancer* 59:12–23.
4. Agerberth B, et al. (1995) FALL-39, a putative human peptide antibiotic, is cysteine-free and expressed in bone marrow and testis. *Proc Natl Acad Sci USA* 92:195–199.
5. Larrick JW, et al. (1995) Human CAP18: A novel antimicrobial lipopolysaccharide-binding protein. *Infect Immun* 63:1291–1297.
6. Larrick JW, Hirata M, Zhong J, Wright SC (1995) Anti-microbial activity of human CAP18 peptides. *Immunotechnology* 1:65–72.
7. Koczulla R, et al. (2003) An angiogenic role for the human peptide antibiotic LL-37/hCAP-18. *J Clin Invest* 111:1665–1672.
8. Shaykhiev R, et al. (2005) Human endogenous antibiotic LL-37 stimulates airway epithelial cell proliferation and wound closure. *Am J Physiol* 289:L842–L848.
9. Heilborn JD, et al. (2003) The cathelicidin anti-microbial peptide LL-37 is involved in re-epithelialization of human skin wounds and is lacking in chronic ulcer epithelium. *J Invest Dermatol* 120:379–389.
10. Cowland JB, Johnsen, AH, Borregaard, N (1995) hCAP-18, a cathelin/pro-bactenecin-like protein of human neutrophil specific granules. *FEBS Lett* 368:173–176.
11. Sorensen OE, et al. (2001) Human cathelicidin, hCAP-18, is processed to the antimicrobial peptide LL-37 by extracellular cleavage with proteinase 3. *Blood* 97:3951–3959.
12. Sorensen OE, et al. (2003) Processing of seminal plasma hCAP-18 to ALL-38 by gastricsin: A novel mechanism of generating antimicrobial peptides in vagina. *J Biol Chem* 278:28540–28546.
13. Yang D, et al. (2000) LL-37, the neutrophil granule- and epithelial cell-derived cathelicidin, utilizes formyl peptide receptor-like 1 (FPRL1) as a receptor to chemoattract human peripheral blood neutrophils, monocytes, and T cells. *J Exp Med* 192:1069–1074.
14. Agerberth B, et al. (2000) The human antimicrobial and chemotactic peptides LL-37 and alpha-defensins are expressed by specific lymphocyte and monocyte populations. *Blood* 96:3086–3093.
15. Studeny M, et al. (2004) Mesenchymal stem cells: Potential precursors for tumor stroma and targeted-delivery vehicles for anticancer agents. *J Natl Cancer Inst* 96:1593–1603.
16. Studeny M, et al. (2002) Bone marrow-derived mesenchymal stem cells as vehicles for intereron-beta delivery into tumors. *Cancer Res* 62:3603–3608.
17. Nakamizo A, et al. (2005) Human bone marrow-derived mesenchymal stem cells in the treatment of gliomas. *Cancer Res* 65:3307–3318.
18. Klopp AH, et al. (2007) Tumor irradiation increases the recruitment of circulating mesenchymal stem cells into the tumor microenvironment. *Cancer Res* 67:11687–11695.
19. Karnoub AE, et al. (2007) Mesenchymal stem cells within tumour stroma promote breast cancer metastasis. *Nature* 449:557–563.
20. Dwyer RM, et al. (2007) Monocyte chemotactic protein-1 secreted by primary breast tumors stimulates migration of mesenchymal stem cells. *Clin Cancer Res* 13:5020–5027.
21. Komarova S, Kawakami Y, Stoff-Khalili MA, Curiel DT, Pereboeva L (2006) Mesenchymal progenitor cells as cellular vehicles for delivery of oncolytic adenoviruses. *Mol Cancer Ther* 5:755–766.
22. Stoff-Khalili MA, et al. (2007) Mesenchymal stem cells as a vehicle for targeted delivery of CRAds to lung metastases of breast carcinoma. *Breast Cancer Res Treat* 105:157–167.
23. Khakoo AY, et al. (2006) Human mesenchymal stem cells exert potent antitumorigenic effects in a model of Kaposi's sarcoma. *J Exp Med* 203:1235–1247.
24. Ramasamy R, et al. (2007) Mesenchymal stem cells inhibit proliferation and apoptosis of tumor cells: Impact on in vivo tumor growth. *Leukemia* 21:304–310.
25. Djouad F, et al. (2003)Immunosuppressive effect of mesenchymal stem cells favors tumor growth in allogeneic animals. *Blood* 102:3837–3844.
26. Tomchuck SL, et al. (2008) Toll-like receptors on human mesenchymal stem cells drive their migration and immunomodulating responses. *Stem Cells* 26:99–107.
27. Zwezdaryk KJ, et al. (2007) Erythropoietin, a hypoxia-regulated factor, elicits a pro-angiogenic program in human mesenchymal stem cells. *Exp Hematol* 35:640–652.
28. Spaeth E, Klopp A, Dembinski J, Andreeff M, Marini F (2008) Inflammation and tumor microenvironments: Defining the migratory itinerary of mesenchymal stem cells. *Gene Ther* 15:730–738.
29. Viswanathan A, Painter RG, Lanson NA, Jr, Wang, G (2007) Functional expression of N-formyl peptide receptors in human bone marrow-derived mesenchymal stem cells. *Stem Cells* 25:1263–1269.
30. Uccelli A, Moretta, L, Pistoia, V (2008) Mesenchymal stem cells in health and disease. *Nat Rev Immunol*, in press.
31. Coffelt SB, Scandurro, AB (2008) Tumors sound the alarmin(s). *Cancer Res* 68:6482–6485.
32. Au P, Tam J, Fukumura D, Jain RK (2008) Bone marrow-derived mesenchymal stem cells facilitate engineering of long-lasting functional vasculature. *Blood* 111:4551–4558.
33. Covas DT, et al. (2008) Multipotent mesenchymal stromal cells obtained from diverse human tissues share functional properties and gene-expression profile with CD146+ perivascular cells and fibroblasts. *Exp Hematol* 36:642–654.
34. Mishra PJ, et al. (2008) Carcinoma-associated fibroblast-like differentiation of human mesenchymal stem cells. *Cancer Res* 68:4331–4339.
35. Beyth S, et al. (2005) Human mesenchymal stem cells alter antigen-presenting cell maturation and induce T-cell unresponsiveness. *Blood* 105:2214–2219.
36. Ren G, et al. (2008) Mesenchymal stem cell-mediated immunosuppression occurs via concerted action of chemokines and nitric oxide. *Cell Stem Cell* 2:141–150.
37. Yotnda P, et al. (2004) Comparison of the efficiency of transduction of leukemic cells by fiber-modified adenoviruses. *Hum Gene Ther* 15:1229–1242.